Chemistry Europe
European Chemical Societies Publishing

Spectroscopic Studies of Synthetic Methylaluminoxane: Structure of Methylaluminoxane Activators

Anuj Joshi,[a] Scott Collins,*[b] Mikko Linnolahti,[c] Harmen S. Zijlstra,[a] Elena Liles,[a] and J. Scott McIndoe*[a]

Abstract: Hydrolysis of trimethylaluminum (Me_3Al) in polar solvents can be monitored by electrospray ionization mass spectrometry (ESI-MS) using the donor additive octamethyltrisiloxane [$(Me_3SiO)_2SiMe_2$, OMTS]. Using hydrated salts, hydrolytic methylaluminoxane (h-MAO) features different anion distributions, depending on the conditions of synthesis, and different activator contents as measured by NMR spectroscopy. Non-hydrolytic MAO was prepared using trimethylboroxine. The properties of this material, which contains incorporated boron, differ significantly from h-MAO. In the case of MAO prepared by direct hydrolysis, oligomeric anions are observed to rapidly form, and then more slowly evolve into a mixture dominated by an anion with *m/z* 1375 with formula $[(MeAlO)_{16}(Me_3Al)_6Me]^-$. Theoretical calculations predict that sheet structures with composition $(MeAlO)_n(Me_3Al)_m$ are favoured over other motifs for MAO in the size range suggested by the ESI-MS experiments. A possible precursor to the *m/z* 1375 anion is a local minimum based on the free energy released upon hydrolysis of Me_3Al.

Introduction

Methylaluminoxane (MAO) is often used as an activator in single-site polymerization catalysis. It serves multiple roles such as scavenging of impurities, alkylation of the catalyst precursor, and ionization to form active catalyst.[1] Despite its useful properties, a large excess is required for high activity in solution[2] and it is rather expensive compared to other alkylaluminoxanes as it is prepared from Me_3Al.[3] Further, residual Me_3Al present in most samples of MAO can have deleterious effects on catalyst activity.[4]

Commercially available MAO formulations are prepared in two main ways – one involves hydrolysis of trimethylaluminum (Me_3Al) in toluene suspension and provides hydrolytic MAO (h-MAO),[3] while the other involves reaction of Me_3Al with C=O compounds, including CO_2 at elevated temperature, to provide non-hydrolytic MAO.[5,6] Various amounts of other trialkylaluminums are added to furnish modified MAO (MMAO).[5] MMAO-12 is a material which is readily available in small amounts that is typically 95 mol% MAO with 5 mol% n-octylaluminoxane incorporated[5] and is thought to be similar to h-MAO with a comparable activator content as measured using donors such as THF and NMR spectroscopy (see Experimental Section for details).[7]

The commercial production of h-MAO is achieved in a continuous process involving intimate mixing of water and a 3–5 fold excess of Me_3Al in dilute toluene suspension.[8] The process is conducted isothermally below room temperature to provide a mixture of h-MAO and unreacted Me_3Al with very little gel formation.[8] Gel formation involves a local excess of water over Me_3Al, as in a suspension, which leads to cross-linking and ultimately formation of a swollen, boehmite gel[9] that incorporates additional water, if present. It is difficult to avoid gel formation in a laboratory setting employing conventional equipment under otherwise identical conditions and with rapid mixing.[10]

Laboratory scale syntheses of h-MAO typically involve the use of hydrated salts in toluene suspension.[11] The salt slowly releases water to the solvent and a controlled hydrolysis is possible. At least initially, a large excess of Me_3Al is also present with respect to dissolved water, although initial methane evolution is often quite vigorous and controlled by the rate of addition of Me_3Al to the salt. Depending on the salt used, gel formation can be minimized, with Li salts providing the highest yields of soluble aluminoxane,[12] compared to an original method developed by Kaminsky and co-workers using $Al_2(SO_4)_3$-$18H_2O$.[13]

Non-hydrolytic MAO (or MMAO) can be prepared on a laboratory scale as documented in the literature.[6] It is prepared at elevated temperature, and as recently reported, MMAO-12 has a very different anion distribution compared to h-MAO when analyzed by ESI-MS using OMTS as a donor additive,

[a] Dr. A. Joshi, Dr. H. S. Zijlstra, E. Liles, Prof. J. S. McIndoe
Department of Chemistry
University of Victoria
3800 Finnerty Road, Victoria BC V8P 5C2 (Canada)
E-mail: mcindoe@uvic.ca

[b] Dr. S. Collins
C/o Department of Chemistry
University of Victoria
3800 Finnerty Road, Victoria BC V8P 5C2 (Canada)
E-mail: scottcol@uvic.ca

[c] Prof. M. Linnolahti
Department of Chemistry
University of Eastern Finland, Joensuu Campus
Yliopistokatu 7, 80100, Joensuu (Finland)

Supporting information for this article is available on the WWW under https://doi.org/10.1002/chem.202100271

despite a similar mechanism of action – *viz* formation of $[Me_2Al(OMTS)]$ $[(MeAlO)_n(Me_3Al)_mMe]$ ion-pairs.[14]

There are other routes to non-hydrolytic MAO such as reaction of Me_3Al with Et_2BOBEt_2[15] or triethylboroxine[16] that proceed at low temperatures, and furnish MAO with very good properties as an activator ($A = 80.7 \times 10^6$ g PE/mol Zr × h × bar at 80 °C at 2500:1 Al:Zr in toluene suspension[16]).[17] Other methods employ organostannoxanes or related compounds as the oxygen source.[18] It would be useful to fully characterize these various materials to determine how they differ from conventional h-MAO, especially since the anion distribution for MMAO-12 (many different anions) could not be more different from that of h-MAO (predominantly one).[14]

The hydrolysis of Me_3Al has been studied in detail, both experimentally and also theoretically. At low temperatures and in a donor solvent, which moderates the hydrolysis reaction, the principal products formed are $(Me_2AlOAlMe_2)_n$ or $Me_2Al(OH)_2AlMe_2$ depending on stoichiometry.[19] The compound $(Me_2AlOAlMe_2)_n$ has never been obtained in pure form, is predominantly trimeric in solution, and is thought to form MAO + Me_3Al when distillation is attempted.[15] $Me_2Al(OH)_2AlMe_2$ is unstable and is said to form MAO in donor solvents but, with unusual characteristics such as 5-coordinate Al, and residual OH groups, and this material is not useful as an activator.[20]

In non-donor solvents, the preparation and composition of MAO has been studied at low temperature using both solvent fractionation and cryoscopy by the group of Sinn and co-workers.[21] They were able to demonstrate that low temperature hydrolysis, involving an excess of Me_3Al, furnished low MW oligomeric material, as would be expected for a classical, step-growth condensation.[22] Sinn invoked aggregation of these materials[19a] via dative Al–O interactions to form higher MW MAO. Based on the reports of Barron and co-workers on the structure of t-butylaluminoxanes,[23] Sinn and co-workers invoked a cage structure formed via aggregation of a linear tetramer (i.e., $Me_2Al(OAMe)_3OAlMe_2$) for the active component of MAO.

Pioneering theoretical work by Zurek and Ziegler examined cage structures for MAO[24b] and also studied the reaction of these cages with Me_3Al,[24a] motivated by the work Barron and co-workers, who demonstrated that Me_3Al was required for catalyst activation using strained, t-butylaluminoxane cages.[25] Other work has shown that models such as nanotubes have comparable stability to classical cages with formula $(MeAlO)_n$.[26] In order for cages to be as stable (per mole repeat unit) they must be of large size so that strained Al_2O_2 rings are minimized.[24,27] Such stable structures reversibly bind only small amounts of Me_3Al.[24a]

Other theoretical work has examined the step-wise hydrolysis of Me_3Al at various levels of theory. One of the few papers to look at both the thermodynamics and dynamics of this process was reported quite some time ago by Hall and co-workers.[28] Glaser and Sun looked at the thermodynamics of various initial steps, motivated by the early experiments of Sinn and other workers, and reached different conclusions about the mechanism of growth in the presence of donors.[29] Linnolahti and co-workers have systematically studied the growth reaction,[30] finally reaching the size of large cages in the size domain of h-MAO (typically 1000–3000 g mol^{-1}).[31]

In a recent paper, we reported ESI-MS experiments aimed at monitoring the formation of h-MAO via hydrolysis of Me_3Al in dilute *o*-difluorobenzene (*o*-$F_2C_6H_4$) and fluorobenzene (PhF) media.[32] Anionic species containing 12–15 aluminum atoms were observed to rapidly form in *o*-$F_2C_6H_4$, with slower transformation to higher MW ions. The final anion distribution was insensitive to experimental conditions such as solvent, and which was dominated by an anion with *m/z* 1375 with composition $[(MeAlO)_{16}(Me_3Al)_6Me]^-$ (hereinafter [**16,6**]$^-$) upon "quenching" with OMTS to form $[Me_2Al(OMTS)]$[**16,6**].

Since this result was similar to ESI-MS analyses previously obtained for samples of commercial h-MAO,[33] we speculated as to the stability of either the precursor or the anion. A new model for this anion was proposed based on a chelated structure. It is much more stable than the previously located cage model for [**16,6**]$^-$.[33c,34]

It should be borne in mind that the component that gives rise to the ion-pair in question comprises no more than 3 mol% of the entire mixture when using this additive.[33a] So, there is little question that most of the neutral aluminoxane present is relatively unreactive. Since neutral methylaluminoxane is likely comprised of many species, it is possible that the precursor which gives rise to [**16,6**]$^-$ is significantly more stable, and/or more reactive than others towards OMTS.

In this paper, we provide full details on these hydrolysis experiments, and interpret some of the transient behaviour seen. We also provide additional experimental data which shows that the anion distribution of h-MAO or non-hydrolytic MAO, as well as other properties can be quite different from that reported previously.[32] In other words, the properties of MAO, including its ion-pair speciation, are largely determined by the conditions and precursors used for synthesis.

Results and Discussion

Anion speciation during hydrolysis

Shown in Figure 1a) is the negative ion ESI-MS of a 2:1 mixture of Me_3Al:H_2O in PhF about 20 minutes after mixing in a magnetically stirred vial containing 0.1 mol% OMTS. The spectrum shows comparable amounts of both low and high MW anions, and low levels of oxidation[35] such that reliable assignments can be made.

In this spectrum the lowest MW anion with any intensity has *m/z* 521 with a likely composition of [**5,3**]$^-$. Another ion [**5,4**]$^-$ appears with variable, but usually lower intensity and is extensively hydrolyzed (Supporting Information Figure S3). The same is also true of [**6,4**]$^-$ (*m/z* 651) which is, however, of greater intensity than either of these, and the most intense anion in this series is [**7,4**]$^-$ under these conditions (excess Me_3Al).

Another spectrum is shown in Figure 1b) at the same conversion but with only 20 mol% excess of Me_3Al present. The appearance of this spectrum is different from the 2:1 ratio

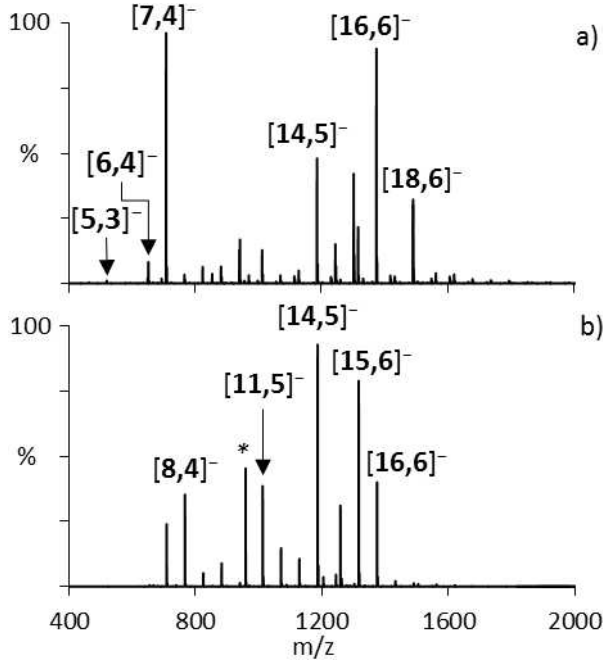

Figure 1. Negative ion ESI-MS of a) a mixture of Me_3Al (0.064 M) and wet PhF ($[H_2O] = 0.032$ M) in the presence of 0.1 mol% OMTS after 20 minutes b) $[Me_3Al] = 0.038$ M after 34 minutes with major anions labelled. * An ion with *m/z* 959 contains one fluorine.

employed for the first. In particular anion [**8,4**]$^-$ is now the most intense anion seen at low *m/z* ratios, while a new anion with *m/z* 959 is especially prominent.

MS/MS studies confirm that *m/z* 959 has one equivalent of Me_2AlF incorporated (Supporting Information Figure S4) and is likely related to the classical anion [**10,5**]$^-$. Small amounts of other ions, presumably related to this one were seen in both solvents as evidenced by enhanced intensity for the M+4 isotopomers relative to the parent ion for the aluminoxane anions.

Evidently, there is reaction of electrophilic Me_2Al-species with a fluorine source, either the solvent or an impurity, occurring in solution. In fact, a species formed from commercial MAO, and formulated as $[Me_2Al(o\text{-}F_2C_6H_4)]^+$ was detected by NMR spectroscopy in this solvent some years ago by Bochmann and co-workers.[7a] We have not detected this species by ESI-MS under any conditions, nor the PhF analogue, suggesting that they are not stable to the ESI process. However, species of this type may be responsible for formation of Me_2AlF, especially in the absence of stronger donors such as OMTS.[36] As we have also seen ion fluorination in connection with other, unrelated reactions and it is definitely occurring in the gas phase[37] we cannot completely rule out formation of these fluorinated anions via ion-molecule reactions in the source compartment, involving the solvent or another fluorinated impurity.[38]

Oxidation, or specifically the presence of Me_2AlOMe in the Me_3Al used, has an impact on the appearance of the ESI-MS (Supporting Information Figure S1). More importantly, it has a decisive influence on the change in the anion speciation with time. Shown in Figure 2 are ESI-MS from two experiments in $o\text{-}F_2C_6H_4$ under the same conditions at the same time where one was conducted with pure Me_3Al and the other with material contaminated with about 1 mol% Me_2AlOMe (determined by ^1H NMR spectroscopy).

It is obvious that the growth reaction leading predominantly to [**16,6**]$^-$ has been largely arrested in the presence of the latter material. Since the total amount of activator in commercial h-MAO is typically on the order of 1–3 mol% depending on how it is measured[33a] it is very likely that oxidation, or specifically Me_2AlOMe is inhibiting formation of a key intermediate or intermediates involved in the growth process.

In the absence of oxidation, the changes in anion speciation in the two different solvents are similar, though there are obvious differences in rate and conditions under which the reaction reaches completion (defined as no perceptible change in anion distribution with time). As shown in Figure 3 in Ph-F a 2-fold or more excess of Me_3Al over water is needed to drive the reaction to completion at room temperature, while in $o\text{-}F_2C_6H_4$ the entire process is much faster (*vide infra*) and only a slight excess of Me_3Al results in completion, regardless of whether OMTS is present or not during hydrolysis.[32]

These experiments were conducted with solvents that had been distilled under N_2, saturated with water at room temperature and then degassed using a freeze-pump-thaw procedure. The water content was measured through reaction of an aliquot with Cp_2ZrMe_2.[39] For experiments summarized here, the measured water content in PhF varied between 0.009 and

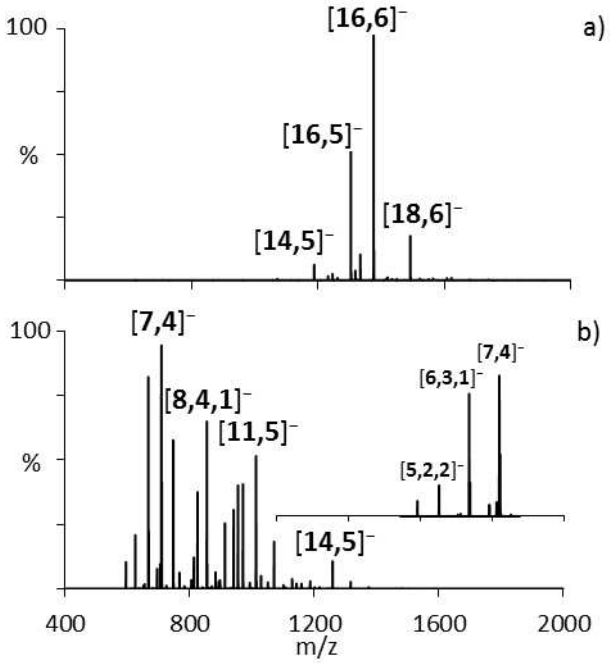

Figure 2. ESI-MS of hydrolyzed Me_3Al in $o\text{-}F_2C_6H_4$ a) after 40 min. b) after 40 min but using oxidized Me_3Al. Some of the oxidized anions with composition $[(MeAlO)_n(Me_3Al)_m(Me_2AlOMe)_oMe]^-$ have been previously assigned by MS/MS;[35] inset shows expansion of low *m/z* region with tentative assignments.

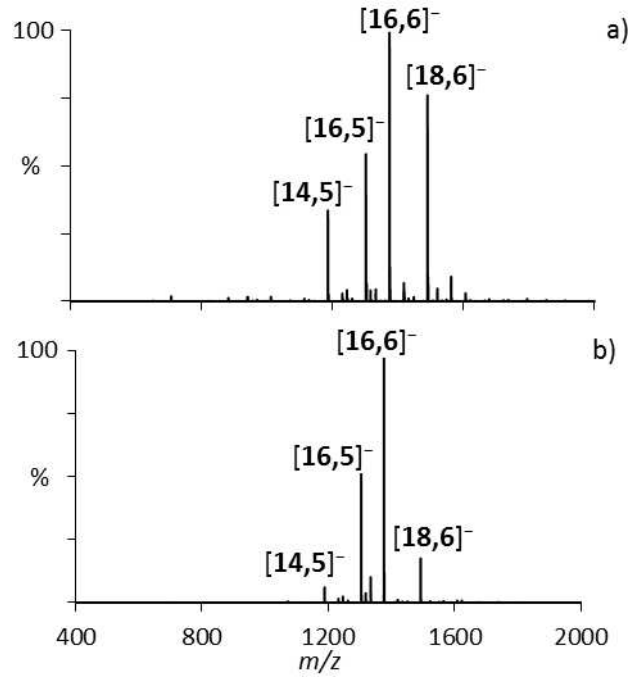

Figure 3. ESI-MS of hydrolyzed Me_3Al in a) PhF and b) *o*-$F_2C_6H_4$ upon completion of the growth reaction. For conditions, see Figure 1a) and Ref. [32]. The increased intensity of [**16,5**]$^-$ relative to [**16,6**]$^-$ in these spectra results in part from source-induced fragmentation (see Supporting Information p. 2).[38]

0.032 M while for *o*-$F_2C_6H_4$ a higher water content (0.055 M) was determined.

The equilibrium solubility of water in various aromatic halo- and hydrocarbon solvents are <0.02 M for all studied including PhF (0.0175 M).[40] The equilibrium solubility of water in *o*-$F_2C_6H_4$ does not appear to have been determined. However, the aqueous solubility of this solvent and PhF are very similar (0.010 and 0.016 M, respectively), as are the free energies of hydration (-3.1 and -3.4 kJ mol^{-1}) and other measures of aqueous solubility (e.g., Henry's constant and K_{ow}).[41]

As such, experiments in the two solvents at $[H_2O] > 0.018$ M likely proceed with water in suspension to varying degrees. This means that one is actually looking at competing homogeneous and heterogeneous reactions, and so the product distribution will be quite sensitive to experimental conditions, including initial stoichiometry.

A ^{1}H NMR spectrum of the *o*-$F_2C_6H_4$ mixture about 24 hours at room temperature following completion of monitoring, revealed the presence of a mixture of Me_3Al and only low MW aluminoxane (Supporting Information, Figure S5). This counter-intuitive result can be explained by competing formation of boehmite gel,[9] possibly in a hydrated state [i.e., $Al(OH)_3$]. In other words, the local excess of water present in suspension diverts some of the Me_3Al added to $Al(OH)_3$ or related species, and this requires a 3:1 O:Al stoichiometry for complete conversion of Al–C bonds. The organic phase thus becomes enriched in Me_3Al relative to dissolved water. Evidently, from the NMR spectrum only a very small fraction of the final mixture is soluble, high MW MAO while ESI-MS is a sufficiently sensitive technique that the oligomerization process can still be monitored.

Reaction Monitoring

Two different procedures were used to monitor these reactions. In PhF solvent, small amounts of OMTS were added at the start with either continuous monitoring or withdrawal of aliquots by syringe – so-called *in situ* conditions. The other procedure involved withdrawal of aliquots and "quenching" with OMTS, usually 1 mol% – so-called *ex situ* methods, involving off-line data analysis. A continuous version of the *ex situ* process was adopted for experiments in *o*-$F_2C_6H_4$.[32]

The changes in composition in PhF are illustrated in Figure 4 for individual anions. First, low MW anions with the composition [**n,4**]$^-$ (n = 6–10) dominate the mass spectra at early reaction times, while during growth the anions with compositions [**14,m**]$^-$, [**15,m**]$^-$ and [**16,m**]$^-$ (m = 5–6) are typically more abundant than anions with lower n.

In *o*-$F_2C_6H_4$ the reaction is significantly more rapid, even after accounting for the differences in $[H_2O]$ and $[Me_3Al]$. The changes depicted in Figure 4 are complete within 10 minutes at room temperature, while the composition of the mixture changes from dynamic to largely static.

The basic features are shown in Figure 5. Here, one sees formation of predominantly [**15,5**]$^-$ and [**15,6**]$^-$ (as well as [**14,5**]$^-$ and [**14,6**]$^-$), which decay forming [**16,5**]$^-$ and [**16,6**]$^-$ as well as higher MW anions such as [**18,6**]$^-$. This slower process dominates the changes in composition at longer times.

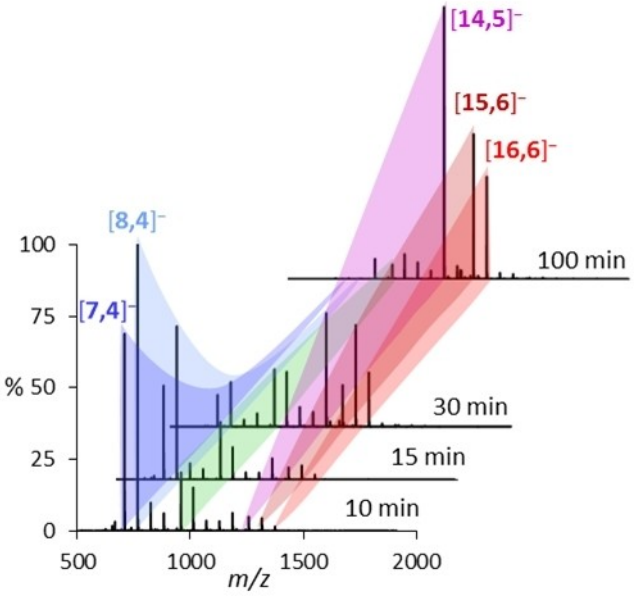

Figure 4. Trends in anion intensities with time in PhF. For conditions see Figure 1b).The intensity of the fluorinated anion with *m/z* 959 is highlighted in green, and its relative intensity is not changing to the same extent.

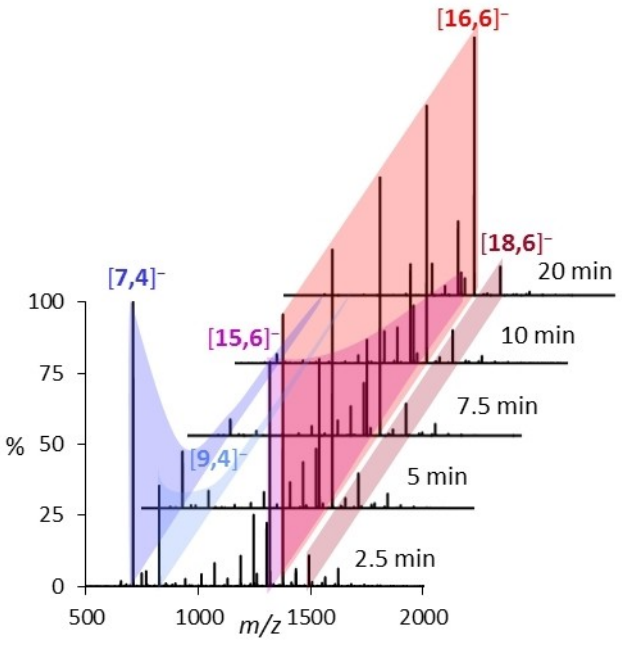

Figure 5. Ion intensities vs. time in *o*-$F_2C_6H_4$. For conditions see Ref. [32].

In both solvents the average *m/z* ratio of the mixture changes in the manner shown in Figure 6.[32] For the different reactions which have been studied, this change does not follow simple exponential growth but instead is better described by bi-exponential growth (see Supporting Information for details).In other words there are at least two stages, one rapid and the other slower, that characterize the change in composition of the mixture with time.[42]

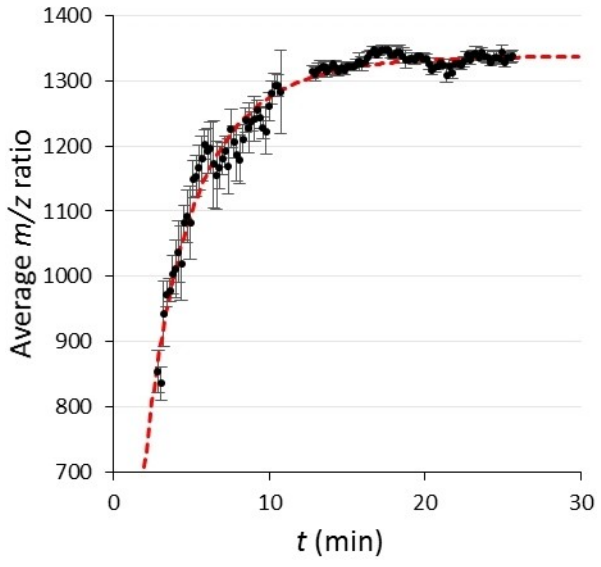

Figure 6. Average m/z ratio vs. time for reaction of Me_3Al with water (Al:O = 1.2:1 [H_2O] = 0.055 M) in *o*-$F_2C_6H_4$ in the presence of 0.2 mol% OMTS. Raw data has been averaged every ten points, with error bars representing the standard deviation of those points. The data has been fit to the sum of two exponential functions (see Supporting Information p. 6).

Analysis of this data show that the limiting *m/z* ratio upon completion is inversely dependent on [Me_3Al] but not in a dramatic fashion as would otherwise be expected for a step-growth process.[22] OMTS does not have an effect on the final *m/z* ratio, but the slow growth process is impeded when this material is present. Finally, slow growth appears solvent dependent, being significantly faster in *o*-$F_2C_6H_4$ than in PhF (Supporting Information).

It is interesting to note that of the various additives we have studied, only OMTS stabilizes commercial MAO from gelation or aging.[43] We suspect that slow growth is related to that process, and which appears to involve low MW oligomers likely present in MAO such as $(MeAlO)_1(Me_3Al)_3$ or $(MeAlO)_2(Me_3Al)_4$ (**1,3** or **2,4**, respectively).[30,31] In earlier work, the initial aging process involves conversion of [**16,6**]$^-$ to *inter alia* [**18,6**]$^-$ in commercial material,[33b] while similar behaviour is seen here (e.g. Supporting Information Figure S2 and S6).

It is worth pointing out that the hydrolysis of Me_3Al is essentially a diffusion controlled process in the initial stages.[28] None of the monitoring experiments, even under the most dilute conditions, capture those steps, which are largely complete on mixing. Even the initial rapid appearance of low MW anions (minutes in *o*-$F_2C_6H_4$) are due to chemically activated processes with significant barriers ($\triangle G^{\ddagger} > 80$ kJ mol^{-1} at 298 K with [H_2O] = 0.055 M).

Evidently, the formation of aluminoxane activators involves several different, but slower processes occurring at somewhat different rates. One of these could involve incremental growth through step-wise reaction of lower MW species with an oligomer, or as proposed previously, mutual reaction of higher MW species with each other.[32] In fact, it is possible there is more than one way to form a particular reactive species, and/or that there are different, reactive species with the same composition formed by different routes. These species would be indistinguishable by mass spectrometry. A great deal of caution is required in relating the monitoring experiments to an underlying mechanism, especially since ion intensity in ESI-MS is due to many factors other than solution concentration.[44]

ESI-MS analysis of preparative aluminoxane syntheses

We studied formation of h-MAO using salt hydrates and also looked at the reaction of trimethylboroxine with Me_3Al to compare that product to h-MAO. These reactions were not convenient for reaction monitoring due to their heterogeneous nature. However, we wondered whether the ESI-MS of high MW MAO would differ from that seen using commercial vs. synthetic material.

The original procedure reported by Kaminsky was followed using a 2:1 H_2O:Al ratio and $Al_2(SO_4)_3 \cdot 18H_2O$.[13] It should be noted that in the structure of this salt, twelve of the eighteen water molecules in the unit cell are coordinated to two Al atoms in octahedral fashion, while the remaining six molecules are lattice water.[45] It is known that thermal dehydration of this

salt proceeds in stages, with only two H_2O being easily lost at temperatures below 85 °C, and ten additional H_2O between that temperature and 177 °C.[46] We expect that between two to twelve H_2O are readily available for reaction with Me_3Al at room temperature in toluene suspension. Thus, the stated 2:1 reaction actually corresponds to a 4.5-fold excess to 0.75 equiv. of Me_3Al with respect to available water. It would be otherwise impossible to prepare high MW, soluble aluminoxane in good yield at a 2:1 H_2O:Al ratio.[22]

As is documented in the literature, this preparation involves an initial, vigorous reaction that produces methane at a rate that requires a controlled addition of Me_3Al to this salt on a preparative scale. The total amount of methane initially produced never exceeds that expected (i.e., 2 moles per mole of available water), though formation of insoluble material (i.e., gel) is problematic if an uncontrolled addition is employed. After the initial rapid reaction, methane continues to slowly evolve until the theoretical amount is produced (based on Me_3Al used).

This procedure was followed on a mmol scale using an internal standard 1,3,5-tri-*t*-butylbenzene. Aliquots were withdrawn at early times after rapid methane evolution had ceased, and as described in the literature after about 20 hr, and were filtered prior to analysis. The filtered aliquots were analyzed by both ESI-MS in PhF and by ^1H NMR spectroscopy, after addition of excess THF, to determine conversion, Me_3Al and $[Me_2Al(THF)_2]^+$ content according to the procedures in the literature.[7] NMR spectra are provided as Supporting Information while the preparative and analytical results are summarized in Table 1.

In the case of LiOH-H_2O, a similar procedure to that used for aluminum sulphate was adopted (i.e., using an excess of Me_3Al with respect to water[12]) however, this reaction is strongly exothermic, and the temperature could not be controlled within the confines of a glovebox. The mixtures were analyzed by NMR and ESI-MS after the initial exotherm had abated and upon cooling to room temperature (ca. 3 hrs) and on stirring overnight at room temperature.

Extended reaction times resulted in a decrease in yield of soluble aluminoxane (70% or lower), and the Li salt was fouled with reactive aluminoxane based on vigorous methane evolution on hydrolysis.

Of the two salt hydrolyses investigated, only the Al salt provides MAO whose ESI-MS strongly resembles that of a commercial sample (Figure 7a), and it was also the only sample to exhibit a detectable signal for $[Me_2Al(THF)_2]^+$ in the corresponding NMR spectrum in THF (Figure S9b).

The Li salt provided MAO with a different anion distribution as shown in Figure 7b) after 24 h. It is dominated by the higher MW anions [**18,7**]$^-$ and [**18,6**]$^-$, though some [**16,6**]$^-$ is present. The spectrum is very similar to one reported for 10 wt%

Table 1. Preparation of MAO, Me_3Al and activator content.

Entry	Precursor	t [hr]	Yield[a]	Me_3Al [mol%]	$[Me_2Al(L)]^+$[mol%]	L
1	$Al_2(SO_4)_3$-18H_2O	3	>90	33.5	0.30	THF_2
2	$Al_2(SO_4)_3$-18H_2O	20	71	12.5	0.19	THF_2
3	$Al_2(SO_4)_3$-18H_2O	3	16[b]	13.0	0.53	THF_2
4	$Al_2(SO_4)_3$-18H_2O	20	55[b]	12.7	0.31	κ^2-$(RO)_2SiMe_2$
5	LiOH-H_2O	3	>90	9.3	0.0	THF_2
6	LiOH-H_2O	3	65[b]	11.0	1.0	κ^2-$(RO)_2SiMe_2$
7	LiOH-H_2O	24	44	18.7	0.0	THF_2
Entry	Precursor	t (hr)	Yield[a]	Me_3Al (mol%)	$[Me_2Al(L)]^+$(mol%)	O_2BMe (mol%)[c]
8[d]	c-$(OBMe)_3$	3	>90	20.4[g]	0.0	19.5[g]
9[e]	c-$(OBMe)_3$	3	70	0.0	0.0	8.8
10[f]	c-$(OBMe)_3$	3	20	0.0	0.0	15.0

[a] Total soluble Al including Me_3Al using 1,3,5-tri-t-butylbenzene as an internal standard, except where noted. [b] Isolated yield of soluble MAO and residual Me_3Al. [c] mol% O_2BMe groups determined from integration of NMR spectra in THF-toluene. [d] Trimethyboroxine (1.0 equiv.) added to 6 equiv. of Me_3Al at room temperature. [e] Trimethyboroxine (1.0 equiv.) added to 3.3 equiv. of Me_3Al at room temperature. [f] Me_3Al (3.3 equiv.) added to 1.0 equiv. of trimethylboroxine. [g] NMR spectrum dominated by $(Me_2AlOBMe_2)_n + Me_3Al$.

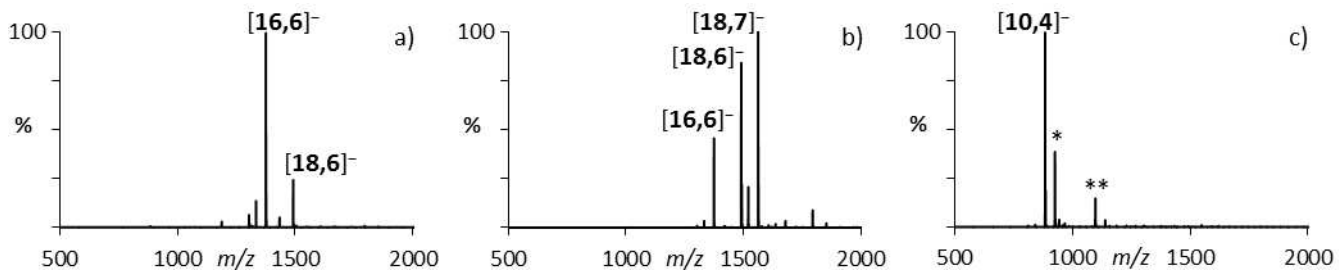

Figure 7. ESI-MS of synthetic MAO samples in PhF with 1 mol% OMTS a) from Al salt after 20 hr (Table 1, entry 2) b) from Li salt after 20 hr (Table 1, entry 7) c) from trimethylboroxine after 3 hr at room temperature (Table 1, entry 9). Ions with a * and ** contain 1 and 2, B atoms, respectively.

Albemarle MAO after several weeks aging at room temperature.[33b] Both samples prepared from the Al or Li salt exhibited signs of aging at room temperature after 20–24 hours (Supporting Information and Figures S2 and S6). Also, a cation with Li incorporated was detected in the corresponding positive ion ESI-MS (Figure S11); it is known that this MAO contains small amounts of Li.[47]

As mentioned above, no $[Me_2Al(THF)_2]^+$ activator signal was evident in the corresponding NMR spectrum (Figure S9a), while in the presence of silicone grease, which is reactive towards MAO in the same fashion as OMTS,[33a,d] signals due to $[Me_2Al(L)]^+$ ($L = \kappa^2$-$(OR)_2SiMe_2$, $R = (SiMe_2O)_n$) are present in both the Al and Li samples (Figure S10) and indicate reactive components present at 0.31 and 1.0 mol%, respectively.

The reaction of trimethylboroxine with Me_3Al was conducted in a similar manner to that reported in the patent literature using triethylboroxine, and as reported there,[16] gelation was observed depending on the order and rate of addition. Gel formation was minimal when trimethylboroxine was slowly added to a significant excess of Me_3Al. Under these conditions (Table 1, entry 8) the yield of soluble material was extremely high, approaching a quantitative yield by NMR. Lower yields were obtained with some gel produced if the same procedure was used with a near-stoichiometric ratio (Table 1, entry 9). The lowest yields were obtained when Me_3Al was added to trimethylboroxine (Table 1, entry 10).

The ESI-MS are again different, and some of the anions contain boron (Figure 7c, Figure S12). MS/MS studies on the ion with *m/z* 925 indicate that the boron is lost as BMe_3 (Figure S13). On this basis, this ion can be assigned a composition of $[\mathbf{11,3}(BMe_3)Me]^-$ though it is unlikely that boron is incorporated as BMe_3 *per se*.

The ESI-MS of these mixtures was quite variable and reflect variable moisture content in the solvents used for this preparative work. In essence, the MAO formed from the boroxine precursor is not very reactive towards OMTS while that formed by hydrolysis of Me_3Al is (Figure S14).

Under optimal conditions (i.e., addition of boroxine to a slight excess of Me_3Al) very little free Me_3Al was present and no $[Me_2Al(THF)_2]^+$ was detected either by NMR spectroscopy while $MeBO_2$ or Me_2BO moieties are present in the product (Figure S15).

It is intriguing that depending on the method of synthesis that the Me_3Al and $[Me_2Al]^+$ activator content (as measured using THF as donor) of synthetic MAO can differ significantly. That prepared from trimethylboroxine is depleted in Me_3Al and $[Me_2Al]^+$ activator content under optimal conditions (slight excess of Me_3Al), and yet is competent to activate metallocene catalysts.[16] Also, h-MAO that is chemically depleted of excess Me_3Al is well known to function as an effective activator, and often with much higher efficacy.[4] Even the neutral precursor speciation appears important with respect to the availability of $[Me_2Al]^+$ using THF vs. chelating donors such as OMTS,[33a] or silicone grease. Evidently, different methods of activation are possible, including the original concept of alkylation (by MAO vs. Me_3Al) and subsequent ionization via Me^- abstraction involving Lewis acidic sites present in MAO depleted of Me_3Al.[48]

Finally, these preparative data conclusively illustrate that the ESI-MS of the hydrolysis experiments reported here and earlier[32] reflect the specific conditions of this reaction (possibly isothermal, dilute solution or suspension). Theoretical work (*vide infra*) suggests the neutral precursor to $[\mathbf{16,6}]^-$ represents a local rather than a global minimum. Indeed, this *has to be the case*, otherwise there would be no driving force for the aging of MAO, which is accompanied by formation of higher MW anions, such as $[\mathbf{18,6}]^-$ and ultimately gelation.[33,49]

Theoretical results – sheet structures for MAO activators

As mentioned in the introduction, Linnolahti and co-workers have studied the formation of MAO, using the M06-2X[50]/TZVP[51] method as implemented in Gaussian 16[52] to the size range suggested by experiment (MW ~1000–3000 g mol^{-1}).[31] For neutral molecules with the formula $(MeAlO)_n(Me_3Al)_m$ they predicted that chain or ring molecules would be favoured for low n, while sheets were favoured in the size range $n = 5$–12 with a transition to cage structures at $n \sim 13$. The most stable cage located by theory had the formula $(MeAlO)_{16}(Me_3Al)_6$ (**16,6**) in apparent agreement with the early ESI-MS results.[33]

In more recent work, where a targeted search focused on free energy, we find that sheets are more stable than cages, provided sufficient Me_3Al is available to stabilize them through binding along their reactive edges – so-called structural Me_3Al.[53]

Shown in Figure 8 are the new results in terms of ΔG-c/*n* for sheets with $n = 6$–18. The gas phase *G* values are corrected to condensed phase (*G*-c) with the *TS* term scaled by 2/3,[54,55] and

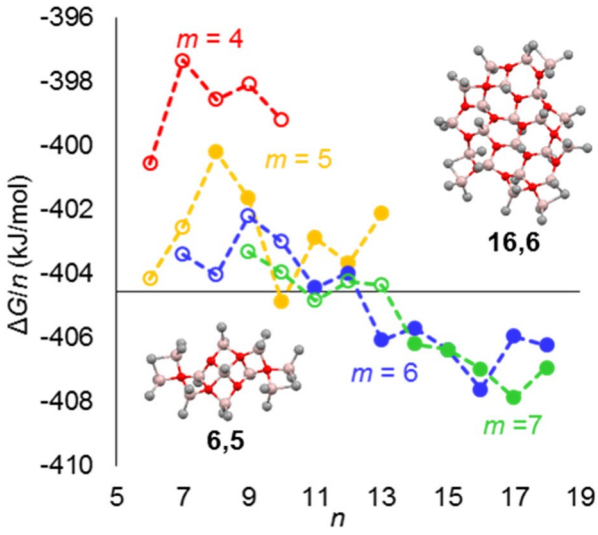

Figure 8. ΔG-c/*n* values for MAO sheets as a function of *n* and *m* with structures of more stable 5- and 4-coordinate sheets shown. Open circles correspond to 5-coordinate, while filled circles to 4-coordinate sheets. The x-axis is located at the ΔG-c/*n* value for the most stable cage **16,6** previously located.[31]

ΔG-c/n values are for the reaction $0.5\times(n+m)$ $Me_6Al_2 + n$ $H_2O \rightarrow (MeAlO)_n(Me_3Al)_m + 2n$ CH_4 at $T = 298$ K and $p = 1$ atm.

For lower MW sheets, structures with 5-coordinate Al and strained, four-membered Al_2O_2 rings are stable (open circles Figure 8) while higher MW sheets feature 4-coordinate Al and six-membered Al_3O_3 rings (closed circles in Figure 8). At intermediate sizes both types of structures have comparable energies, for example for **9,6**, 5- and 4-coordinate sheets differ in ΔG-c by 1.8 kJ mol^{-1}.

Based on the magnitude of ΔG-c/n the larger sheets are clearly favoured on a thermodynamic basis, and **16,6** and **17,7** are local minima for $m = 6$ and 7, respectively on this basis. However, ΔG-c/n reflects the free energy change for hydrolysis of Me_3Al based upon the moles of water consumed. It is not a measure of global thermodynamic stability (except in the case of isomers). Other metrics, such as the free energy change per mole of Me_3Al ($n+m$), result in a different ordering of these structures, with **18,6** the lowest energy sheet on this basis. This is easy to understand as this sheet features the lowest Me_3Al content in its size range. Indeed, based on earlier work,[27,56] an infinite aluminoxane sheet consisting of six-membered rings is expected to be the global minimum in terms of stability.

If we review the $\triangle G$-c/n data in Figure 8 the most stable 5-coordinate sheets have the compositions **6,5**, **7,6** and **8,6**, while **9,7** is somewhat higher in $\triangle G$-c/n. These neutrals could serve as precursors for the ions we detect at early stages, though they would have to ionize by $[Me_2Al]^+$ abstraction, with the resulting ions easily prone to loss of Me_3Al in solution or though in-source fragmentation reactions. In contrast, meta-stable, intermediate 4-coordinate sheets include **10,5**, **11,6**, **13,6** and **14,7** in that order based on $\triangle G$-c. Only the anion $[\mathbf{14,5}]^-$ is reasonably intense in both the intermediate and final ESI-MS spectra (Figure 1 and 3). We do detect $[\mathbf{14,6}]^-$ with variable intensity, so it is possible that it fragments to form $[\mathbf{14,5}]^-$ in the source compartment. The final anion distribution is dominated by $[\mathbf{16,6}]^-$ under isothermal conditions consistent with the neutral precursor being **16,6** or somewhat less stable **16,7**.

As for aging, we have not yet studied the kinetics nor mechanism of that process in detail. In the specific case of conversion of e.g., **15,6** to **16,6** involving **1,2** (Figure 9) the process is definitely favoured based on G-c but may feature a significant barrier given that Al–C bonds must be broken (and reformed) to incorporate this fragment into the sheet.

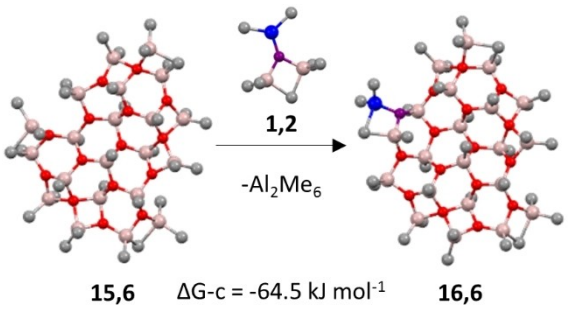

Figure 9. Aging of **15,6** to produce **16,6**. Hydrogen atoms omitted for clarity with Al atoms in pink, O atoms in red and C atoms in grey, except for **1,2** where the Al (blue) and O (purple) are incorporated into the product as shown.

Conclusions

Synthetic methylaluminoxane differs significantly in the ion-pairs which form from this material and donors like OMTS in polar media as revealed by ESI-MS. Moreover, the reactivity of the synthetic MAO towards different donors also differs significantly as revealed by NMR spectroscopy. In particular, organoboron precursors furnish MAO with both low levels of Me_3Al and with boron incorporated as revealed by both techniques. The properties of synthetic MAO are a function of precursor (i.e. hydrolytic vs non-hydrolytic) as well as the conditions for synthesis such as temperature. The growth of ion-pair precursors can be monitored by ESI-MS and is characterized by at least two growth processes that differ in their rate. The slower process appears to be related to initial aging of MAO, which appears to involve a low MW oligomer that incorporates into the larger sheets. Theoretical studies on the hydrolysis of Me_3Al suggest the neutral precursor to $[\mathbf{16,6}]^-$ represents a local rather than a global minimum; at lower temperatures one would predict (as is observed) that hydrolytic MAO should feature this precursor as a kinetic product. Future theoretical work will focus on the stability of even larger structures as well as provide insight into formation of these structures and whether or not sheets are eventually transformed into cages or other structures. We also hope to provide insight into activator stability vs. reactivity which would be helpful in more closely relating theory to experiment. Finally, it would be interesting if the pronounced differences we see in anion speciation had implications for polymerization catalysis.

Experimental Section

General: Trimethylaluminum solution (2.0 M in toluene), trimethylboroxine, octamethyltrisiloxane (OMTS) and hydrated salts were obtained from Sigma Aldrich and used as received. Fluorobenzene (PhF) was obtained from Oakwood Chemicals Ltd. refluxed and distilled from CaH_2 and stored over activated molecular sieves 4 Å prior to use. Toluene (HPLC grade) was dried and purified by passage through activated alumina under N_2 using an MBraun Solvent Purification System or by distillation from Na and benzophenone and stored over activated molecular sieves 4 Å prior to use. Tetrahydrofuran was purified by passage through alumina, or via distillation from K and benzophenone, and stored over activated molecular sieves 4 Å prior to use. All preparative experiments were conducted using Schlenk techniques on a double manifold line under N_2 or Ar or in an MBraun glove-box in stirred vials.

Warning! The direct reaction of Me_3Al with water in hydrocarbon suspension is violently exothermic, with the possibility of explosion and injury to personnel and/or damage to equipment if one reagent is added rapidly to the other. The synthesis of MAO requires a controlled hydrolysis on the laboratory scale, and specialized equipment and process control on a commercial scale. Do not attempt to scale up any of the procedures used for

monitoring the hydrolysis in dilute fluoroarene solution or suspension by ESI-MS.

Synthesis of MAO – $Al_2(SO_4)_3 \cdot 18H_2O$:[13] In a typical procedure, 2.5 mL of a 2.0 M Me_3Al solution (5.0 mmol) was added drop-wise *via* syringe to a rigorously degassed, suspension of the hydrated salt (366 mg, 0.55 mol = 9.89 mmol H_2O) in toluene (2.5 mL) in a magnetically stirred vial inside a glove-box. After vigorous CH_4 evolution had subsided, the reaction mixture was filtered, using a vacuum dried, 0.2 μ PP syringe filter, washing with 2×2.5 mL of toluene. A portion of the filtrate was analyzed by NMR in THF to determine the yield of soluble aluminoxane. An aliquot was treated with 1 mol% OMTS in dry PhF and then diluted to ca. [Al] = 0.01 M using additional dry PhF for analysis by ESI-MS.

Preparative experiments were conducted outside the glove-box using Schlenk techniques on a double manifold with oven dried glassware. In one experiment, the preparative reaction was conducted for 3 h at room temperature prior to filtration using a small, double-tube Schlenk vessel with glass frit. The yield of soluble aluminoxane was 16% while a ^{1}H NMR spectrum showed a Me_3Al content of 10.6 mol% after removal of solvent and excess Me_3Al. For a representative ESI-MS prior to filtration and isolation see Figure 7a). In another experiment the yield of soluble aluminoxane was 55% after 20 hr (literature 63%)[13] while a ^{1}H NMR spectrum showed 0.2 mol% $[Me_2Al(THF)_2]^+$ and 12.5 mol% Me_3Al. For comparison to a commercial sample, see Figure S9.

$LiOH \cdot H_2O$: The procedure reported by Sangokoya[12] was modified as follows: A suspension of $LiOH \cdot H_2O$ (400 mg, 9.53 mmol) in 5 mL of dry toluene containing 100 mg of 1,3,5-tri-t-butylbenzene was rigorously degassed using three, freeze-pump-thaw cycles on a vacuum line. The suspension was transferred into a glove-box under vacuum. A solution of Me_3Al in toluene (5.0 mL of 2.0 M, 10.0 mmol) was added via syringe over 5 min. Gas was evolved and the mixture became warm during this addition. The resulting suspension was heated at 60 °C for about 30 min. After 2 hours at room temperature the mixture was filtered using a syringe filter, washing with 2×0.5 mL of dry toluene. A 1 mL aliquot was removed and analyzed by ESI-MS and NMR. For typical ESI-MS spectra of this material see Figure 7b). A ^{1}H NMR spectrum of this material (see Figure S9a) had a Me_3Al content of 9.3 mol% and recovery of soluble Al of roughly 100%. The remaining filtrate was concentrated *in vacuo* to afford a solid foam (0.398 g, 65% yield).

In some of the NMR work, the distilled THF solvent used for sample preparation was contaminated with silicone grease. As shown in Figure S10, under these conditions the resonance due to silicone grease is split into two peaks, and an additional sharp resonance is seen to lower field of that due to Me_3Al-THF. The integrated ratio of the latter to lower field $SiMe_2$ signal was always 1:1 consistent with formation of $[Me_2Al(L)]^+$ where $L = \kappa^2$-$(RO)_2SiMe_2$ [$R = (OSiMe_2)_n$]. In these cases, the activator content was calculated based on the ratio of the Me_2Al^+ resonance with respect to bulk MAO and Me_3Al-THF. As expected, that value is higher than what one typically measures using THF. See Ref. [33a] for analogous studies using OMTS and other donors.

Trimethylboroxine: The procedures of Wellborn[16] were adopted with the following changes: 1,3,5-tri-*t*-butylbenzene (110 mg) was used as an internal standard and 284.4 mg (2.27 mmol) of trimethylboroxine were dissolved in 2.7 mL of toluene. This stock solution was divided into three equal parts (~1.0 mL each).

1) The first part was added drop-wise via syringe over 30 min to a rapidly stirred solution of Me_3Al in toluene (1.2 mL, 2.0 M, 2.40 mmol). After stirring for 2.5 hours the clear but viscous solution was analyzed by ESI-MS and NMR using THF. If the boroxine was added more rapidly, variable amounts of a gel phase formed and the yield of soluble aluminoxane was significantly lower.
2) The second part was rapidly stirred while 1.2 mL of Me_3Al in toluene was added drop-wise via syringe. The solution turned cloudy and with visible gel forming on the walls of the vial. After 2.5 hours it was filtered, with difficulty, using a 0.2 μ PP syringe filter, washing with toluene.
3) The third part was added over 30 minutes to a 6-fold excess of Me_3Al (2.27 mL of 2.0 M). This preparation was gel-free.

NMR spectra of these mixtures in the presence of 80 vol% THF are shown in Figure S15. Representative ESI-MS of these filtered solutions are shown in Figure S12 and Figure S14. A prominent ion with one boron was analyzed by MS-MS, that spectrum appears in Figure S13.

ESI-MS Experiments: In a typical procedure, a stock solution (~3 mL) was prepared from synthetic MAO (0.75 mL of ~1.0 M) and the amount of a PhF solution of OMTS (0.5 mL of 0.015 M) needed to give an Al:OMTS ratio of ~100:1. After mixing, the stock solution was further diluted with PhF so as to provide a final solution ca. 0.02 M in Al. This solution was analyzed using a QTOF Micro spectrometer via pumping it at ca. 40 μL/min through PTFE tubing (1/16" o.d., 0.005" i.d.) to the ESI-MS probe and source using a syringe pump. Capillary voltage was set at 2900 V with source and desolvation gas temperature at 85 °C and 185 °C, respectively with the desolvation gas flow at 400 L/h. MS/MS data were obtained on product ion spectra using argon as the collision gas and a voltage range of 2–100 V.

For an experiment involving observing ion intensity vs. time, 2 mL of Me_3Al in PhF (0.032 M), containing 0.1 mol% OMTS was added to 1 mL of "wet" degassed PhF ($[H_2O] = 0.032$ M as measured by NMR using Cp_2ZrMe_2[39]) with rapid stirring. An aliquot was withdrawn via gas-tight syringe, and the solution pumped at 40 μL/min into the QTOF Micro source compartment.

Analysis of synthetic MAO samples by NMR spectroscopy: The samples were initially analyzed by NMR as described in the literature using THF as an additive. In the original paper by Imhoff and co-workers, a 4:1 v:v ratio of THF:MAO solution (10–30 wt%) was recommended for determination of Me_3Al content.[7b] In subsequent work, various molar Al:THF ratios were employed to determine both Me_3Al content and $[Me_2Al(THF)_2]^+$ content using a 30 wt% commercial MAO formulation.[7a] When we first started trying to characterize the various synthetic samples prepared using a 5:1 to 10:1 THF:Al mole ratio, as suggested by the results of Ghiotto and co-workers,[7a] we noticed that the position of the Me_3Al-THF resonance was quite variable (using benzene-d_6 as lock solvent), while many hydrolytic samples lacked a resolved signal due to $[Me_2Al(THF)_2]^+$.

Using a sample of 30 wt% MAO from Albemarle and diluted with both toluene and two different levels of Me_3Al (total [Al] = 1.0 M) we discovered that the chemical shift of Me_3Al-THF resonance was a linear function of solvent composition, while that due to $[Me_2Al(THF)_2]^+$ was less variable (typically seen at δ −0.75 ppm). A working curve is shown in Figure S16. Basically, in order to see separate signals due to both $[Me_2Al(THF)_2]^+$ and Me_3Al-THF, with the latter well-resolved from the main resonance of MAO, one should be working at least 75 vol% of THF with respect to MAO solution, regardless of dilution or the Me_3Al content of the latter. In samples with Me_3Al content that differ strongly from a commercial sample (i.e., usually much higher), higher amounts of THF are beneficial for resolving the Me_3Al-THF signal which shifts to higher field with increasing amounts of THF. Our results confirm the original work reported by Imhoff and co-workers.[7b] We include a spectrum of MMAO-12 obtained from Sigma Aldrich for comparison

purposes in Figure S17. This sample has almost twice the activator content as a typical sample of h-MAO.

Computational details: Calculations were carried out by Gaussian 16 software,[52] using the M06-2X metahybrid GGA functional of the Minnesota series[50] combined with the def-TZVP basis set by Ahlrichs *et al.*[51] Harmonic vibrational frequencies were calculated to confirm the structures either as a true minimum or a transition state on the potential energy surface. Gibbs free energies were calculated at $T = 298$ K and $p = 1$ atm and were corrected for condensed phase (ΔG-c) by multiplication of the $T\Delta S$ term of Gibbs free energy by 2/3, as recommended and used in the previous literature.[31,54,55]

The sheet structures of the MAOs were located by systematically following the TMA hydrolysis reactions, as described previously.[30] We note that the approach may not reflect the eventual formation mechanism of the sheets (which is not yet precisely known), and as such, may include structural alternatives that are of limited experimental relevance. In this work, we specifically focused on sheet structures, following the reactions separately for both 4- and 5-coordinate structures, which is not straightforward, as in many compositions the two structural types have a capability of interconverting into each other. The reaction paths were followed based on condensed phase corrected Gibbs free energies. We note here that in our previous report reaching the same size domain[31] we made the choice based on total electronic energy, with a generalized assumption that entropies of isomers are approximately equal. However, it turns out the entropies of sheets are systematically about 6% higher than the entropies of cages having the same composition, which plays in favour of sheets due to the $T\Delta S$ term of Gibbs energy, leading to the preference of sheets over cages within the investigated size range.

Acknowledgements

J.S.M. thanks NSERC (Strategic Project Grant #478998-15) and NOVA Chemicals' Centre for Applied Research for operational funding and CFI, BCKDF, and the University of Victoria for infrastructural support. A.J. thanks the University of Victoria for a graduate fellowship and the Nora and Mark Degoutiere Memorial Scholarship. S.C. acknowledges support for a Visiting Scientist position from the University of Victoria, and also support from Dra. Odilia Pérez-Camacho, Centro de Investigación en Química Aplicada, Saltillo, COAH, MX in connection with a research visit. Thanks to Mr. Christopher Barr of the Department of Chemistry for help with some NMR experiments. M.L. acknowledges computer capacity from the Finnish Grid & Cloud Infrastructure (urn:nbn:fi:research-infras 2016072533).

Conflict of Interest

The authors declare no conflict of interest.

Keywords: ESI-MS · methylaluminoxane · NMR · sheet structures · synthesis

[1] a) H. S. Zijlstra, S. Harder, *Eur. J. Inorg. Chem.* **2015**, 19–43; b) M. Bochmann *Organometallics* **2010**, *29*, 4711–4740.
[2] a) M. E. Z. Velthoen, A. Muñoz-Murillo, A. Bouhmadi, M. Cecius, S. Diefenbach, B. M. Weckhuysen, *Macromolecules* **2018**, *51*, 343–355 and references therein; b) W. Kaminsky, *Macromolecules* **2012**, *45*, 3289–3297.
[3] D. B. Malpass in *Handbook of Transition Metal Polymerization Catalysts*, (Eds.: R. Hoff, R. T. Mathers), Wiley, New York, **2010**, p. 1–28.
[4] a) F. Zaccaria, C. Zuccaccia, R. Cipullo, P. H. M. Budzelaar, A. Macchioni, V. Busico, C. Ehm, *Eur. J. Inorg. Chem.* **2020**, 1088–1095; b) V. Busico, R. Cipullo, R. Pellecchia, G. Talarico, A. Razavi, *Macromolecules* **2009**, *42*, 1789–1791; c) V. Busico, R. Cipullo, F. Cutillo, N. Friederichs, S. Ronca, B. Wang, *J. Am. Chem. Soc.* **2003**, *125*, 12402–12403.
[5] G. M. Smith, S. W. Palmaka, J. S. Rogers, D. B. Malpass, *U. S. Patent 5,831,109*, **1998**, 5 pp.
[6] a) Y. Okajima, Y. Nakayama, T. Shiono, R. Tanaka, *Eur. J. Inorg. Chem.* **2019**, 2392–2395; b) A. F. R. Kilpatrick, J.-C. Buffet, P. Nørby, N. H. Rees, N. P. Funnell, S. Sripothongnak, D. O'Hare, *Chem. Mater.* **2016**, *28*, 7444–7450; c) T. Dalet, H. Cramail, A. Deffieux, *Macromol. Chem. Phys.* **2004**, *205*, 1394–1401.
[7] a) F. Ghiotto, C. Pateraki, J. Tanskanen, J. R. Severn, N. Luehmann, A. Kusmin, J. Stellbrink, M. Linnolahti, M. Bochmann, *Organometallics* **2013**, *32*, 3354–3362; b) D. W. Imhoff, L. S. Simeral, S. A. Sangokoya, J. H. Peel, *Organometallics* **1998**, *17*, 1941–1945.
[8] a) J. K. Roberg, R. E. Farritor, E. A. Burt, *U. S. Patent 5,599,964*, **1997**, 8 pp; b) J. K. Roberg, E. A. Burt, *U. S. Patent 5,663,394*, **1997**, 12 pp.
[9] a) C. J. Harlan, M. R. Mason, A. R. Barron, *Organometallics* **1994**, *13*, 2957–2969; b) C. C. Landry, J. A. Davis, A. W. Apblett, A. R. Barron, *J. Mater. Chem.* **1993**, *3*, 597–602; c) A. W. Apblett, A. C. Warren, A. R. Barron, *Chem. Mater.* **1992**, *4*, 167–182.
[10] a) A. Storr, K. Jones, A. W. Laubengayer, *J. Am. Chem. Soc.* **1968**, *90*, 3173–3177; b) E. J. Vandenberg, *J. Polym. Sci.* **1960**, *47*, 486–489.
[11] S. S. Reddy, S. Sivaram, *Progress in Polymer Science* **1995**, *20*, 309–367.
[12] S. A. Sangokoya, *U. S. Patent 5,041,583*, **1991**, 4 pp.
[13] W. Kaminsky, H. Hahnsen, *U. S. Patent 4,544,762*, **1985**, 4 pp.
[14] H. S. Zijlstra, A. Joshi, M. Linnolahti, S. Collins, J. S. McIndoe, *Dalton Trans.* **2018**, *47*, 17291–17298.
[15] K. Kacprzak, J. Serwatowski, *Appl. Organometal. Chem.* **2004**, *18*, 394–397.
[16] H. C. Welborn, Jr. *U. S. Patent 4,952,714*, **1990**, 6 pp.
[17] See also a) R. Tanaka, T. Hirose, Y. Nakayama, T. Shiono, *Polymer J.* **2016**, *48*, 67–71; b) B. Richter, A. Meetsma, B. Hessen, J. H. Teuben, *Angew. Chem. Int. Ed.* **2002**, *41*, 2166–2169; *Angew. Chem.* **2002**, *114*, 2270–2273; c) B. Richter, A. Meetsma, B. Hessen, J. H. Teuben, *Chem. Commun.* **2001**, 1286–1287.
[18] a) Y. V. Kissin, A. J. Brandolini, *Macromolecules* **2003**, *36*, 18–26; b) S. J. Obrey, A. R. Barron, *J. Chem. Soc. Dalton Trans.* **2001**, 2456–2458.
[19] a) S. Pasynkiewicz, *Polyhedron* **1990**, *9*, 429–453; b) M. Bolesławski, J. Serwatowski, *J. Organomet. Chem.* **1983**, *255*, 269–278; c) M. Boleslawski, J. Serwatowski, *J. Organomet. Chem.* **1983**, *254*, 159–166.
[20] Y. Kimura, S. Tanimoto, H. Yamane, T. Kitao, *Polyhedron* **1990**, *9*, 371–376.
[21] a) H. Sinn, *Macromol. Symp.* **1995**, *97*, 27–52; b) H. Winter, W. Schnuchel, H. Sinn, *Macromol. Symp.* **1995**, *97*, 119–125.
[22] A. Rudin, *The Elements of Polymer Science and Engineering 2nd Ed.*, Academic Press, London, **1999**, pp. 155–188.
[23] a) C. J. Harlan, S. G. Bott, A. R. Barron, *J. Am. Chem. Soc.* **1995**, *117*, 6465–6474; b) M. R. Mason, J. M. Smith, S. G. Bott, A. R. Barron, *J. Am. Chem. Soc.* **1993**, *115*, 4971–4984.
[24] a) Z. Falls, N. Tymińska, E. Zurek, *Macromolecules* **2014**, *47*, 8556–8569; and references therein; b) E. Zurek, T. Ziegler, *Prog. Polym. Sci.* **2004**, *29*, 107–148.
[25] M. Watanabi, C. N. McMahon, C. J. Harlan, A. R. Barron, *Organometallics* **2001**, *20*, 460–467 and references therein.
[26] a) M. Linnolahti, J. R. Severn, T. A. Pakkanen, *Angew. Chem. Int. Ed.* **2008**, *47*, 9279–9283; *Angew. Chem.* **2008**, *120*, 9419–9423; b) M. Linnolahti, J. R. Severn, T. A. Pakkanen, *Angew. Chem. Int. Ed.* **2006**, *45*, 3331–3334; *Angew. Chem.* **2006**, *118*, 3409–3412.
[27] M. Linnolahti, T. N. P. Luhtanen, T. Pakkanen, *Chem. Eur. J.* **2004**, *10*, 5977–5987.
[28] L. Negureanu, R. W. Hall, L. G. Butler, L. A. Simeral, *J. Am. Chem. Soc.* **2006**, *128*, 16816–16826.
[29] R. Glaser, X. Sun, *J. Am. Chem. Soc.* **2011**, *133*, 13323–13336.
[30] a) J. T. Hirvi, M. Bochmann, J. R. Severn, M. Linnolahti, *ChemPhysChem* **2014**, *15*, 2732–2742; b) M. Linnolahti, A. Laine, T. A. Pakkanen, *Chem. Eur. J.* **2013**, *19*, 7133–7142.
[31] M. Linnolahti, S. Collins *ChemPhysChem.* **2017**, *18*, 3369–3374.

[32] A. Joshi, H. S. Zijlstra, E. Liles, C. Concepcion, M. Linnolahti, J. S. McIndoe, *Chem. Sci.* **2021**, *12*, 546–551.
[33] a) H. S. Zijlstra, A. Joshi, M. Linnolahti, S. Collins, J. S. McIndoe, *Eur. J. Inorg. Chem.* **2019**, 2346–2355; b) H. S. Zijlstra, M. Linnolahti, S. Collins, J. S. McIndoe, *Organometallics* **2017**, *36*, 1803–1809; c) T. K. Trefz, M. A. Henderson, M. Linnolahti, S. Collins, J. S. McIndoe *Chem. Eur. J.* **2015**, *21*, 2980–2991; d) T. K. Trefz, M. A. Henderson, M. Wang, S. Collins, J. S. McIndoe, *Organometallics* **2013**, *32*, 3149–3152.
[34] S. Collins, M. Linnolahti, M. G. Zamora, H. S. Zijlstra, M. T. R. Hernández, O. Perez-Camacho, *Macromolecules* **2017**, *50*, 8871–8884.
[35] H. S. Zijlstra, S. Collins, J. S. McIndoe, *Chem. Eur. J.* **2018** *24*, 5506–5512.
[36] a) L. Oliva, P. Oliva, N. Galdi, C. Pellecchi, L. Sian, A. Macchioni, C. Zuccaccia, *Angew Chem. Int. Ed.* **2017**, *56*, 14227–14231; *Angew. Chem.* **2017**, *129*, 14415–14419; b) M. Klahn, C. Fischer, A. Spannenberg, U. Rosenthal, I. Krossing, *Tetrahedron Lett.* **2007**, *48*, 8900–8903.
[37] A. Joshi, H. S. Zijlstra, S. Collins, J. S. McIndoe, *ACS Catalysis* **2020**, *10*, 7195–7206.
[38] A. Joshi, S. Donnecke, O. Granot, D. Shin, S. Collins, I. Paci, J. S. McIndoe, *Dalton Trans.* **2020**, *49*, 7028–7036.
[39] N. A. Yakelis, R. G. Bergman, *Organometallics* **2005**, *24*, 3579–3581.
[40] J. Wing, W. H. Johnston, *J. Am. Chem. Soc.* **1957**, *79*, 864–865.
[41] M. J. S. Monte, A. R. R. P. Almeida, *Chemosphere* **2017**, *189*, 590–598 and references therein.
[42] It is known that the controlled hydrolysis of excess Et_3Al features at least two underlying rates of ethane elimination. See S. Amdurski, C. Eden, H. Feilchenfeld, *J. Inorg. Nucl. Chem.* **1961**, *23*, 133–134.
[43] S. A. Sangokoya, *U. S. Patent 5,731,253* **1998** 10 pp.
[44] I Omari, P Randhawa, J Randhawa, J Yu, J. S. McIndoe, *J. Am. Soc. Mass Spec.* **2019**, *30*, 1750–1757.
[45] X. Sun, Y. Sun, J. Yu, *Cryst. Res. Technol.* **2015**, *50*, 293–298.
[46] G. K. Çılgı, H. Cetişli, *J. Thermal Anal. Calorimetry* **2009**, *98*, 855.
[47] S. A. Sangokoya, *US Patent 5,922,631*, **1999**, 9 pp.
[48] F. Zaccaria, C. Zuccaccia, R. Cipullo, P. H. M. Budzelaar, A. Macchioni, V. Busico, C. Ehm, *ACS Catal.* **2019**, *9*, 2996–3010.
[49] H. S. Zijlstra, M. C. A. Stuart, S. Harder, *Macromolecules* **2015**, *48*, 5116–5119.
[50] Y. Zhao, D. G. Truhlar, *Theor. Chem. Acc.* **2008**, *120*, 215–241.
[51] A. Schäfer, C. Huber, R. Ahlrichs, *J. Chem. Phys.* **1994**, *100*, 5829–5835.
[52] M. J. Frisch *et al.* Gaussian 16, Revision B. 01. **2016**, Gaussian Inc, Wallingford CT. (46AD).
[53] a) F. Zaccaria, P. H. M. Budzelaar, R. Cipullo, C. Zuccaccia, A. Macchioni, V. Busico, C. Ehm, *Inorg. Chem.* **2019**, *59*, 5751–5759; b) D. E. Babushkin, N. V. Semikolenova, V. N. Panchenko, A. P. Sobolev, V. A. Zakharov, E. P. Talsi, *Macromol. Chem. Phys.* **1997**, *198*, 3845–3854; c) I. Tritto, C. Méalares, M. C. Sacchi, P. Locatelli, *Macromol. Chem. Phys.* **1997**, *198*, 3963–3977.
[54] S. Tobisch, T. Ziegler *J. Am. Chem. Soc.* **2004**, *126*, 9059–9071.
[55] C. Ehm, G. Antinucci, P. H. M. Budzelaar, V. Busico, *J. Organomet. Chem.* **2014**, *772–773*, 161–171 and references therein.
[56] M. Linnolahti, A. J. Karttunen, T. A. Pakkanen, *ChemPhysChem* **2006**, *7*, 1661–1663.

Manuscript received: January 22, 2021
Accepted manuscript online: March 29, 2021
Version of record online: May 11, 2021

